



Microwave calcaneus phantom for bone imaging applications

Title	Microwave calcaneus phantom for bone imaging applications
Author(s)	Amin, Bilal;Kelly, Daniel;Shahzad, Atif;O'Halloran, Martin;Elahi, Muhammad Adnan
Publication Date	2020-03-15
Publisher	Institute of Electrical and Electronics Engineers
Repository DOI	10.23919/EuCAP48036.2020.9135355

Microwave calcaneus phantom for bone imaging applications

Bilal Amin^{1,2}, Daniel Kelly³, Atif Shahzad^{2,3}, Martin O'Halloran^{1,2,3}, Muhammad Adnan Elahi^{1,2}

¹Electrical and Electronic Engineering, National University of Ireland Galway, Ireland, b.amin2@nuigalway.ie

²Translational Medical Device Lab, National University of Ireland Galway, Ireland

³School of Medicine, National University of Ireland Galway, Ireland

Abstract—Microwave imaging can be used as an alternate modality for monitoring bone health. Dielectrically accurate, anthropomorphic phantoms play vital role in testing of imaging prototype prior to clinical applications. However, no study to date has proposed cortical and trabecular bone phantoms. This paper presents a multilayered 3D-printed human calcaneus structure. Further, we have proposed liquid based tissue phantoms that mimic the dielectric properties of skin, muscle, cortical bone and trabecular bone. Tissue phantoms are composed of Triton X-100, water and salt. The dielectric properties were measured across 0.5 – 8.5 GHz. Each layer of the 3D-printed structure was filled with corresponding tissue phantom. The combined average percentage difference between dielectric properties of reference data and proposed tissue phantoms was found to be 2.9% for trabecular bone, 7.3% for cortical bone, 7.1% for muscle, and 8.7% for skin over the full measured frequency band. These tissue phantoms and 3D printed human calcaneus structure can be used as a valuable test platform for microwave diagnostic studies.

Index Terms—microwave imaging, tissue phantoms, dielectric properties, bone health, Triton X-100.

I. INTRODUCTION

The dielectric properties (namely relative permittivity and conductivity) of biological tissues characterize the interaction of electromagnetic (EM) waves with tissue [1]. These properties are considered as key parameters for the development of various EM diagnostic and therapeutic medical devices [2]. Microwave imaging (MWI) has received a significant attention as a diagnostic technology for diagnosing various diseases [3]. MWI exploits the dielectric contrast of the tissues at target anatomical site [4] and diagnoses the disease based on the difference of dielectric properties between healthy and diseased tissues [5]. MWI has made significant progress towards breast cancer detection [6] and for the diagnosis of brain stroke [7]. The clinical advantages of MWI technology are: portability, low cost and non-ionizing nature of the radiation that provides a safe alternative to several existing imaging technologies for diagnostic and monitoring [5],[8]. Besides breast cancer detection, MWI has been recently proposed to measure *in vivo* dielectric properties of human calcaneus for osteoporosis monitoring [3],[9]. Studies have shown that notable contrast exists between dielectric properties of healthy and diseased bone samples [10]. This contrast can be exploited by using MWI. Therefore, MWI can be employed for monitoring bone health as an alternative or supplementary technology to the Dual-energy X-ray Absorptiometry (DXA) and Computed Tomography (CT) [3], [8], [11]. Prior to clinical testing of MWI device for *in vivo* dielectric properties assessment, tissue phantoms (TPs) are used to mimic the

dielectric properties of tissues for device validation. A few studies have proposed the TPs for homogeneous single-structures of bone for the applications of brain stroke detection [12][13], however, to the best of authors' knowledge, no tissue phantom (TP) has been proposed that mimics the dielectric properties of cortical bone and trabecular bone separately.

Phantoms emulate dielectric properties of different human body parts and are crucial component in the testing and development of MWI systems. Ideally, the reference phantoms should be anatomically and dielectrically accurate whilst being easily produced and time stable. Oil-in-gelatine TPs have been widely used to emulate breast tissues and are attractive due to their ease of fabrication and their capacity to simulate the dielectric properties of a wide range of tissues [14]. One major weakness of oil-in-gelatine TPs is their sensitivity to environmental exposure, which over time, causes desiccation [5]. Alternatively, carbon black mixtures also show potential as a TP due to their flexibility, dielectric stability and mechanical strength [15]. Hence, carbon black based solid mixtures provide phantoms that are stable over time, however, these TPs are hard to reconfigure to account changes associated with appearance of anatomical lesion compared to liquid based TPs [5].

Triton X-100 appears to be an excellent candidate for a liquid based phantom due to its better relative heat stability (allowing to perform experiments at room as well as human body temperature) and due to the fact that its dielectric properties have been shown to be stable for up to a year [5]. The liquid nature of Triton X-100 solutions ensures that complex structures can be filled by avoiding air bubbles in these structures. Additionally, binary fluid mixture models such as Bottcher's formula can be used to provide an estimate of the permittivity of a given mixture based on sodium chloride and Triton X-100 concentrations [12].

Numerous studies have used 3D-printed breast and head models filled with liquid TPs for MWI prototype testing [16]. Recent advancements in manufacturing technologies has enabled building complex and relatively easily reproducible 3D-printed structures for use in phantom development. One drawback of 3D-printed moulds is the limited choice of

fabricating substrates with acrylonitrile butadiene styrene (ABS) being the most commonly used. The ABS is commonly used despite its electrical permittivity and conductivity is far from the dielectric properties of biological tissue. Therefore, the thickness of these 3D-printed structures should be kept as low as possible to minimize the effect it has on the microwave image [17]. This results in balancing act between rigidity and low field perturbation.

This paper presents a multilayered 3D-printed human calcaneus structure. An imprint of human foot was altered on a 3D-modelling software to obtain a multilayered human calcaneus structure. Each layer represents skin, muscle, cortical bone and trabecular bone. Furthermore, we have proposed Triton X-100 and salt based TPs that mimic the dielectric properties of skin, cortical bone and trabecular bone. These TPs mimic the dielectric properties of considered tissues over 0.5 – 8.5 GHz frequency range. Each layer of 3D-printed structure was filled with respective TP to model human calcaneus. This initial multilayered 3D-printed structure and TPs can be used for microwave imaging of human calcaneus.

II. METHODOLOGY

TPs Preparation

The TPs were prepared by following the procedure outlined in [12]. Based on desired properties, the solution of Triton X-100, water and salt was thoroughly mixed. To create solutions with a wide range of dielectric properties different concentrations of Triton X-100, water and salt concentrations were tested. Higher concentrations of salt were used to increase conductivity whilst higher concentrations of Triton X-100 were used to lower both the conductivity and permittivity of the solutions. As in [5], solutions with Triton X-100 volume in the range of 45-55% became viscous, however, none of the Triton X-100 solutions used in this phantom fell within this range. We have proposed TP for skin, cortical bone and trabecular bone. The Triton X-100 mixture presented in [11] was used for our muscle Triton X-100 solution.

3D-printed structures

3D-modeling software was used to produce a multilayered hollow cylinder model and a calcaneus model based on an imprint of the human foot that was altered to contain three separate chambers. These three chambers would contain our Triton X-100 mixtures for skin, cortical bone and trabecular bone. The dimensions of the inner chambers of the calcaneus model were designed to mimic the dimensions of the cortical and trabecular bone layers of the calcaneus bone [18]. The calcaneus was chosen due to the proximity of the calcaneus bone to the surface and because the ratio of cortical to trabecular bone is similar to that found in the femoral head and lumbar spine [18],[19], which are considered as main scanning sites for osteoporosis monitoring. These models were then printed at 200°C using a PLA filament. The thickness of walls was kept 2mm to prevent leakage of Triton X-100 solutions and to avoid potential low field perturbation.

Dielectric properties measurement

The Open-ended coaxial probe measurement technique was employed in frequency range of 0.5 – 8.5 GHz over 101 linearly

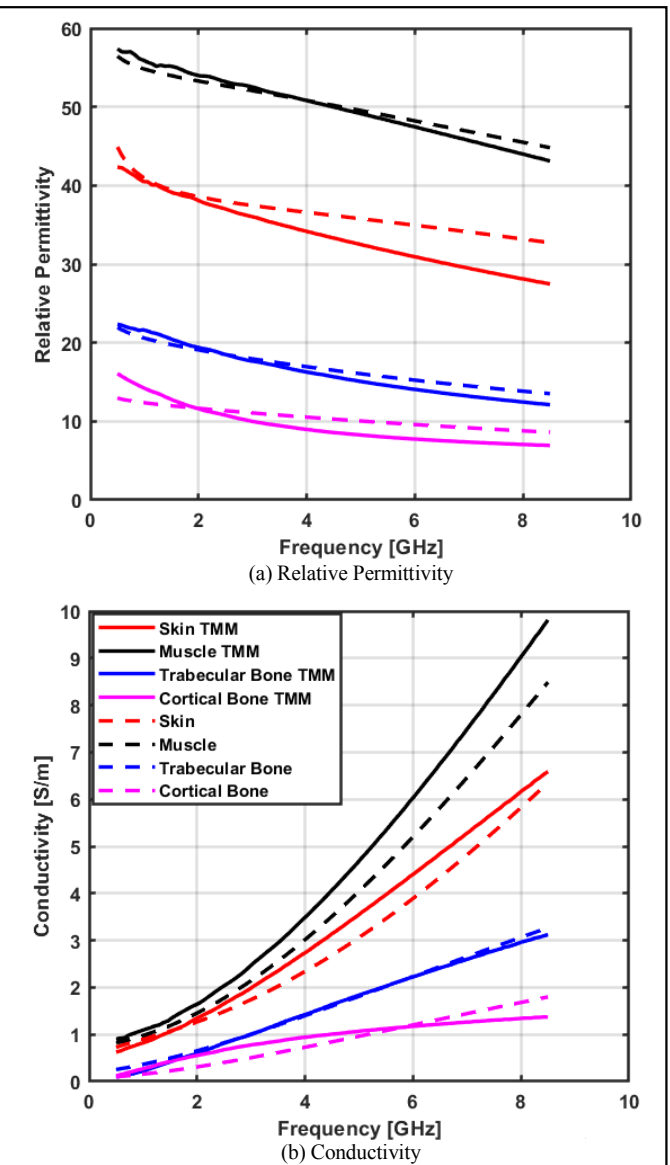


Fig. 1. Dielectric properties of various calcaneus tissues phantoms over 0.5 – 8.5 GHz frequency band. The measured values (solid lines) of TP are compared with reference values from Gabriel *et al.* [21].

spaced points. The Keysight E5063A vector network analyser (VNA) was connected with the Keysight slim form probe 85070E. A standard three-load one-port calibration (Air, Short and Deionized water) was used to calibrate the measurement equipment. The calibration of the measurement equipment was verified by measuring dielectric properties of 0.1 M NaCl solution (saline) [20]. The uncertainty in the accuracy of measurements was found to be 0.047% and 2.7% for relative permittivity and conductivity, respectively.

III. RESULTS AND DISCUSSION

Human calcaneus provides the most suitable anatomical site for MWI due to its peripheral location and similar composition of cortical and trabecular bone to that of femoral head and lumbar spine [11],[12]. The major tissues involved in human calcaneus are the skin, muscle, cortical bone and trabecular

bone. To replicate the dielectric properties of each considered tissue, several TPs containing Triton X-100, salt and water were made. The percentage of Triton X-100 was varied from 90% to 24%. The dielectric properties of all TPs were analysed and the composition of each TP was varied based on difference to the target tissue. Among all TPs four solutions were obtained that mimic the dielectric properties of our target tissues in calcaneus.

Fig. 1 shows the dielectric properties of the Triton X-100 based TPs that mimics the dielectric properties of our target tissues. Each solid curve indicates the mean value of six measurements taken at 101 linearly spaced frequency points between 0.5 – 8.5 GHz. The measurements were obtained at multiple sites in the liquid. The dotted curves represent the corresponding tissue's reference values obtained from Gabriel *et al.* [21]. Gabriel *et al.* [21]'s database is widely used for characterizing the dielectric properties of tissues, therefore we have considered their values for comparison purposes. The composition of TPs that replicate dielectric properties of each investigated tissue is given in Table 1.

The mixture of Triton X-100, water and NaCl was thoroughly mixed before the measurements were performed. The average percentage difference between the dielectric properties of TPs and their respective reference values over 0.5 – 8.5 GHz is calculated for each tissue and is presented in Table 2. The average percentage difference between the dielectric properties of each TP and its respective reference values was found to be less compared to higher frequencies. The low frequency band ranging from 0.5 – 2.4 GHz has more electromagnetic field penetration depth and reduces significantly above 3 GHz. This band is observed to be more feasible for imaging applications of human calcaneus bone.

It can be observed from Fig. 1 (a) and (b), that the mean dielectric properties of TPs mimicking each tissue has a significant overlap with respect to the dielectric properties of reference values. This can be particularly noticed for the relative permittivity graph. But the conductivity of TPs comparatively vary more from reference data in comparison to the relative permittivity specifically for the case of lower conductivity tissues such as cortical bone. Moreover, for cortical bone the relationship between conductivity and frequency is not linear. This effect has been observed due to significant decrease in the amount of water and an increased amount of Triton X-100 in cortical bone's TP compared to other TPs.

The average percentage difference between the dielectric properties of TPs and the reference data of each tissue across 0.5 – 8.5 GHz is given in Table 2. It can be observed from the values of average percentage difference that the relative permittivity profile obtained for each tissue is very much close to the target data in comparison to the conductivity profile data. The average percentage difference between the dielectric properties of TP and its respective tissue is found to be less than $\pm 10\%$, that is the expected variance in biological tissue [22]. The variations observed in results are in agreement to variations reported by studies that proposed TPs for emulating human biological tissues.

It can be observed from Fig. 1 (a) and (b) that except the conductivity profile of cortical bone the measured dielectric properties of each TP are close to reference data for frequencies below 3 GHz. Most microwave tomography imaging systems operate below 3 GHz [11], therefore, considering frequencies above 3 GHz would not be convenient for MWI of trabecular bone.

Table 1. Composition of TX-100 TPs

Target Tissue	TX-100 (vol %)	Water (vol %)	NaCl (g/L)
Skin	40	60	5.2
Muscle	24	76	5
Cortical Bone	77	23	0.8
Trabecular bone	69.5	30.5	0.8

Table 2. Average percentage difference in relative permittivity and conductivity of the TP and respective reference tissue values across 0.5 – 8.5 GHz band

Target Tissue	Relative Permittivity (%)	Conductivity (%)	Combined (%)
Skin	7.8	9.6	8.7
Muscle	0.38	14	7.1
Cortical Bone	9.6	5	7.3
Trabecular Bone	3.4	2.4	2.9

Once the TPs were finalized the 3D structures were printed, the empty layers of the structure were filled with the respective TP to replicate each layer as a tissue. Fig. 2 shows the 3D-printed structures. The yellow structure shows the side and top views of cylindrical phantom, and the blue structure shows the top and bottom views of anatomically accurate calcaneus structure. In order to avoid the problems of leakage, trapped air, and weakness of the structure the thickness of the walls were kept to be 2mm. The yellow structure was designed as our initial test

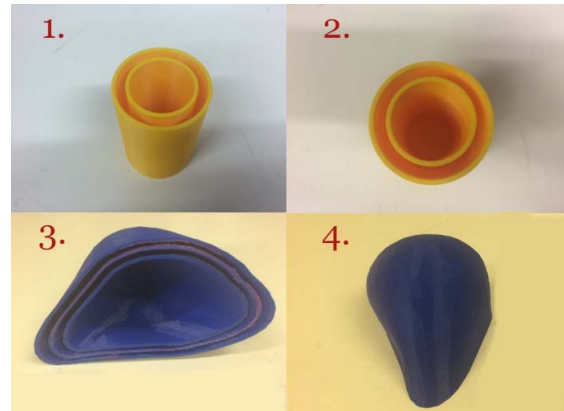


Fig. 2. A view of the 3D-printed components of the phantoms. 1) and 2) Display the multilayered simple cylindrical phantom 3) and 4) Displays the multilayered calcaneus phantom.

case scenario for imaging purposes. As the matter of fact, the calcaneus bone resembles with irregular shaped cylinder, therefore for initial imaging purpose the cylindrical structure can be used.

Conclusion

In this study we have presented a 3D-printed stable reference human calcaneus structure. Moreover, we have proposed TPs that mimic the dielectric properties of skin, muscle, cortical bone and trabecular bone. The TPs were composed of Triton X-100, salt and water. The dielectric properties of TPs were observed across 0.5-8.5 GHz. The multilayers of 3D-printed structure were filled with corresponding TP. The dielectric properties of TPs have shown significant agreement with the reference data. The average percentage difference between relative permittivity of reference data and TP for trabecular bone and cortical bone was found to be 3.4% and 9.6% respectively over the fully observed frequency range. The 3D printed moulds by using STL files enable the fabrication of realistic multilayered structures that can be used to model multilayered phantoms.

The results of dielectric properties of TPs suggest that, the multiple layers of 3D-printed structure can be filled with these TPs and hence provides a feasible and realistic test platform for imaging purposes of bone. These findings motivate the design and development of a MWI based device to measure *in vivo* dielectric properties of bone.

ACKNOWLEDGMENT

The research leading to these results has received funding from the European Research Council under the European Union's Horizon 2020 Programme/ ERC Grant Agreement BioElecPro n. 637780.

REFERENCES

- [1] B. Amin, M. A. Elahi, A. Shahzad, E. Porter, and M. O'Halloran, "A review of the dielectric properties of the bone for low frequency medical technologies," *Biomed. Phys. Eng. Express*, vol. 5, no. 2, p. 022001, 2019.
- [2] B. Amin, M. A. Elahi, A. Shahzad, E. Porter, B. McDermott, and M. O'Halloran, "Dielectric properties of bones for the monitoring of osteoporosis," *Med. Biol. Eng. Comput.*, Aug. 2018.
- [3] P. M. Meaney *et al.*, "Clinical microwave tomographic imaging of the calcaneus: A first-in-human case study of two subjects," *IEEE Trans. Biomed. Eng.*, vol. 59, no. 12, pp. 3304–3313, 2012.
- [4] R. Scapaticci, P. Kosmas, and L. Crocco, "Wavelet-Based Regularization for Robust Microwave Imaging in Medical Applications," *IEEE Trans. Biomed. Eng.*, vol. 62, no. 4, pp. 1195–1202, 2015.
- [5] N. Joachimowicz, B. Duchêne, C. Conessa, and O. Meyer, "Anthropomorphic Breast and Head Phantoms for Microwave Imaging," *Diagnostics*, vol. 8, no. 4, p. 85, 2018.
- [6] E. Porter, M. Coates, and M. Popović, "An Early Clinical Study of Time-Domain Microwave Radar for Breast Health Monitoring," *IEEE Trans. Biomed. Eng.*, vol. 63, no. 3, pp. 530–539, 2016.
- [7] R. Scapaticci, L. Di Donato, I. Catapano, and L. Crocco, "A feasibility study on microwave imaging for brain stroke monitoring," *Prog. Electromagn. Res.*, vol. 40, pp. 305–324, 2012.
- [8] A. H. Golnabi, P. M. Meaney, S. Geimer, T. Zhou, and K. D. Paulsen, "Microwave tomography for bone imaging," *Proc. - Int. Symp. Biomed. Imaging*, vol. 9, pp. 956–959, 2011.
- [9] B. Amin, M. A. Elahi, A. Shahzad, E. Parle, L. McNamara, and M. Orhalloran, "An insight into bone dielectric properties variation: A foundation for electromagnetic medical devices," *EMF-Med 2018 - 1st EMF-Med World Conf. Biomed. Appl. Electromagn. Fields COST EMF-MED Final Event with 6th MCM*, pp. 3–4, 2018.
- [10] B. Amin *et al.*, "Investigating human bone microarchitecture and dielectric properties in microwave frequency range," in *2019 13th European Conference on Antennas and Propagation (EuCAP)*, 2019, pp. 1–5.
- [11] P. M. Meaney, T. Zhou, D. Goodwin, A. Golnabi, E. A. Attardo, and K. D. Paulsen, "Bone dielectric property variation as a function of mineralization at microwave frequencies," *Int. J. Biomed. Imaging*, vol. 2012, 2012.
- [12] N. Joachimowicz, B. Duchene, C. Conessa, and O. Meyer, "Reference phantoms for microwave imaging," *2017 11th Eur. Conf. Antennas Propagation, EUCAP 2017*, pp. 2719–2722, 2017.
- [13] R. Scapaticci, M. Bjelogrlic, J. A. T. Vasquez, F. Vipiana, M. Mattes, and L. Crocco, "Microwave technology for brain imaging and monitoring: physical foundations, potential and limitations," in *Emerging Electromagnetic Technologies for Brain Diseases Diagnostics, Monitoring and Therapy*, Springer, 2018, pp. 7–35.
- [14] M. Lazebnik, E. L. Madsen, G. R. Frank, and S. C. Hagness, "Tissue-mimicking phantom materials for narrowband and ultrawideband microwave applications," *Phys. Med. Biol.*, vol. 50, no. 18, p. 4245, 2005.
- [15] T. Hikage, Y. Sakaguchi, T. Nojima, and Y. Koyamashita, "Development of lightweight solid phantom composed of silicone rubber and carbon nanotubes," in *2007 IEEE International Symposium on Electromagnetic Compatibility*, 2007, pp. 1–4.
- [16] B. L. Oliveira and M. O. Halloran, "Microwave Breast Imaging: Experimental tumour phantoms for the evaluation of new breast cancer diagnosis systems Biomedical Physics & Engineering Related content Microwave Breast Imaging: experimental tumour phantoms for the evaluation of new breast can," no. January, 2018.
- [17] T. Rydholm, A. Phager, M. Persson, S. Geimer, and P. Meaney, "Effects of the Plastic of the Realistic GeePS-L2S-Breast Phantom," *Diagnostics*, vol. 8, no. 3, p. 61, 2018.

- [18] J. M. Vogel, R. D. Wasnich, and P. D. Ross, "The clinical relevance of calcaneus bone mineral measurements: a review," *Bone Miner.*, vol. 5, no. 1, pp. 35–58, 1988.
- [19] B. Clarke, "Normal bone anatomy and physiology.," *Clin. J. Am. Soc. Nephrol.*, vol. 3 Suppl 3, no. Suppl 3, pp. 1–16, 2008.
- [20] C. Gabriel and A. Peyman, "Dielectric measurement: Error analysis and assessment of uncertainty," *Phys. Med. Biol.*, vol. 51, no. 23, pp. 6033–6046, 2006.
- [21] C. Gabriel *et al.*, "The dielectric properties of biological tissues: III . Parametric models for the dielectric spectrum of tissues The dielectric properties of biological tissues: III . Parametric models for the dielectric spectrum of tissues," 1996.
- [22] C. Gabriel, "Dielectric properties of biological tissue: Variation with age," *Bioelectromagnetics*, vol. 26, no. SUPPL. 7, pp. 12–18, 2005.